Magnetic Properties of Uniaxial Synthetic Antiferromagnets for Spin-valve Applications

G. Mankey – University of Alabama

et al.

Citation of published version:

Zhao, Z., et al. (2005): Magnetic Properties of Uniaxial Synthetic Antiferromagnets for Spin-valve Applications. *Physical Review B*, 71(10).
DOI: https://doi.org/10.1103/PhysRevB.71.104417

Magnetic properties of uniaxial synthetic antiferromagnets for spin-valve applications

Zhiya Zhao, P. Mani, and G. J. Mankey*
MINT Center, The University of Alabama, Tuscaloosa, Alabama 35486, USA

G. Gubbiotti
INFM CRS-SOFT, c/o Università di Roma "La Sapienza," I-00185, Roma, Italy and INFM UdR-Perugia, c/o Dipartimento di Fisica, Università di Perugia, Via A. Pascoli, 06123 Perugia, Italy

S. Tacchi
INFM Unità di Perugina and Dipartimento di Fisica, Università di Perugia, Via A. Pascoli, 06123 Perugia, Italy

F. Spizzo
INFM Dipartimento di Fisica dell'Università, Via Paradiso 12, 44100 Ferrara, Italy

W.-T. Lee
Spallation Neutron Source, Oak Ridge National Laboratory, Oak Ridge, Tennessee 37831, USA

C. T. Yu and M. J. Pechan
Miami University, Department of Physics, Oxford, Ohio 45056, USA
(Received 27 July 2004; revised manuscript received 14 December 2004; published 25 March 2005)

The magnetic properties of synthetic antiferromagnetic Si(100)/Ta (5 nm)/Co(t_1)/Ru (0.65 nm)/Co(t_2)/Ta (10 nm) with an obliquely sputtered Ta underlayer are reported as a function of the top Co layer thickness, t_2. The morphological origin of the large in-plane magnetic anisotropy created by the obliquely sputtered Ta underlayer is revealed by atomic force microscopy. The magnetic anisotropy of the base Co layer is determined by measuring the dispersion of the Damon-Eshbach spin-wave mode with Brillouin light scattering. Ferromagnetic resonance measurements and hysteresis loops reveal that both the anisotropy and the saturation field of the trilayer system decrease with increasing top Co layer thickness. The dependence of the saturation field on layer thickness is fitted to an energy minimization equation that contains both bilinear and biquadratic exchange coupling constants. Magnetoresistance and polarized neutron reflectometry results both confirm that the magnetic reversal process of the system is through magnetic domain formation followed by rotation.

DOI: 10.1103/PhysRevB.71.104417 PACS number(s): 75.30.Gw, 75.30.Ds, 73.43.Qt, 75.47.De

Synthetic antiferromagnetic (SyAF) structures consisting of nonmagnetic spacers sandwiched between two ferromagnetic layers have been studied extensively due to their applications in spin-valve (SV) devices, such as read heads and magnetic random access memories (MRAM),[1–3] as well as in recording media.[4] A typical SV device consists of an antiferromagnetic (AF) pinning layer, a SyAF pinned layer, a nonmagnetic spacer layer, and a ferromagnetic free layer.[5] Sensitive response to the external field by a rotation of the magnetization vector of the free layer is crucial to the SV performance. With the rapid shrinking of device dimensions, the magnetostatic interaction between the pinned and free layers becomes significant, degrading the device performance. Using a SyAF structure as either the free layer or the pinned layer has the advantage of producing an adjustable net magnetic moment and reduced magnetostatic interaction between the layers, thus insuring good field sensitivity.

For media applications, no in-plane anisotropy is needed, while in-plane anisotropy is preferred for SV devices.[6] The in-plane magnetic anisotropy that pins the SyAF magnetization is usually induced by the exchange coupling to an AF layer. Large magnetic anisotropy can also be induced by ripple and step structured magnetic films.[7,8] SyAF structures prepared on obliquely sputtered Ta underlayers have large in-plane uniaxial anisotropy due to the pinning effect from the anisotropic roughness of a Ta underlayer.[9,10] Such a SyAF structure can simplify the SV devices by eliminating the AF pinning layer.[11] The purpose of this study is to see if desired properties of SV devices, such as the exchange coupling strength, magnetic anisotropy, magnetic domain structure, and magnetization reversal process, can be achieved by tuning the SyAF structure.

While many efforts have been devoted to study the oscillatory behavior of the interlayer exchange coupling with increasing interlayer thickness, less attention has been given to study the dependence of coupling strength[12] and the in-plane uniaxial anisotropy[13] on the thickness of the ferromagnetic layers. It is important to achieve a better understanding of the effect of changing ferromagnetic layer thickness on the in-plane uniaxial anisotropy, K_u, the coupling strength measured by the saturation field, H_{sat}, associated with the magnetic moment configurations and the switching process of the Co layers.

In a previous paper, we reported that a 0.65-nm Ru thickness resulted in strong and stable interlayer exchange coupling of the Co layers.[10] Here, we report a study of

SyAF structures with varying Co thickness: Si(100)/Ta (5 nm)/Co(t_1)/Ru (0.65 nm)/Co(t_2)/Ta (10 nm). The samples were prepared by sputtering in a system with a base pressure of 5×10^{-9} mbar and a sputtering pressure of 4.5×10^{-3} mbar of ultrapure Ar gas. Film thickness was determined by using a calibrated quartz microbalance. The Ta incidence direction was set at 60° from the sample normal so that the Ta grains grew at a tilted angle, forming a wavy surface. The Co and Ru grains of the subsequent layers grew without a preferred direction.

The surface morphology of the as-deposited Ta underlayer was studied *ex situ* with a Digital Instruments Nanoscope IV atomic force microscopy (AFM). Hysteresis loops were measured by an alternating gradient magnetometer (AGM). Magnetic properties of the samples were measured using Brillouin light scattering (BLS), ferromagnetic resonance (FMR), magnetoresistance (MR) measurement, and polarized neutron reflectometry (PNR). Details of the BLS measurement were reported elsewhere.[13] The FMR measurements were carried out with a rectangular cavity in the transverse electric (TE) 104 mode with the magnetic field applied in the plane of the film. MR data were collected using the van der Pauw configuration with external magnetic field (H_{ext}) parallel to the in-plane magnetic easy axis and the current flowing both perpendicular ($I_\perp$) to the easy axis. PNR measured by a neutron reflectometer, POSY1, at Argonne National Laboratory, was used to determine the magnetic reversal process of the samples.

Figure 1(a) shows the AFM image of an as-deposited 5-nm Ta underlayer. The surface structure resembles one-dimensional waves with an average amplitude of 0.3 nm and an average wavelength of 25 nm with crests and valleys aligned perpendicular to the incidence direction of the Ta flux. Figure 2(a) shows the dispersion of the Damon-Eshbach (DE)[14] mode as a function of the in-plane direction of the external magnetic field. Distinguishable easy-axis (EA) and hard-axis (HA) hysteresis loops of the Co underlayer are shown in the insets. The EA ($\Phi=0°$) is along the crests' and valleys' direction and perpendicular to the Ta incidence direction while the HA ($\Phi=90°$) lies along the projection of the Ta incidence direction onto the substrate surface.

To further investigate the in-plane magnetic anisotropy, BLS measurements have also been performed by changing the intensity of the magnetic field along the EA ($\Phi=0°$) and the HA ($\Phi=90°$). The results of these measurements are reported in Fig. 2(b). Along the EA, the spin-wave frequency (solid dots) decreases with external field, while along the HA (open dots), there is a local minimum in the frequency at an external field of about 1 kOe followed by a field range where the frequency is almost constant. This is typical hard-axis behavior, and indicates a reorientation of the magnetization for a field of about 1 kOe. In fact, upon reducing the strength of the external field, the magnetization does not remain oriented along the hard in-plane direction and starts to rotate towards the nearest in-plane easy direction. To determine the uniaxial in-plane anisotropy, K_u, and the out-of-plane anisotropy, K_s, both the DE frequency dependence on the in-plane direction of the applied field, as well as that on the intensity of the external field, were simultaneously fitted keeping the

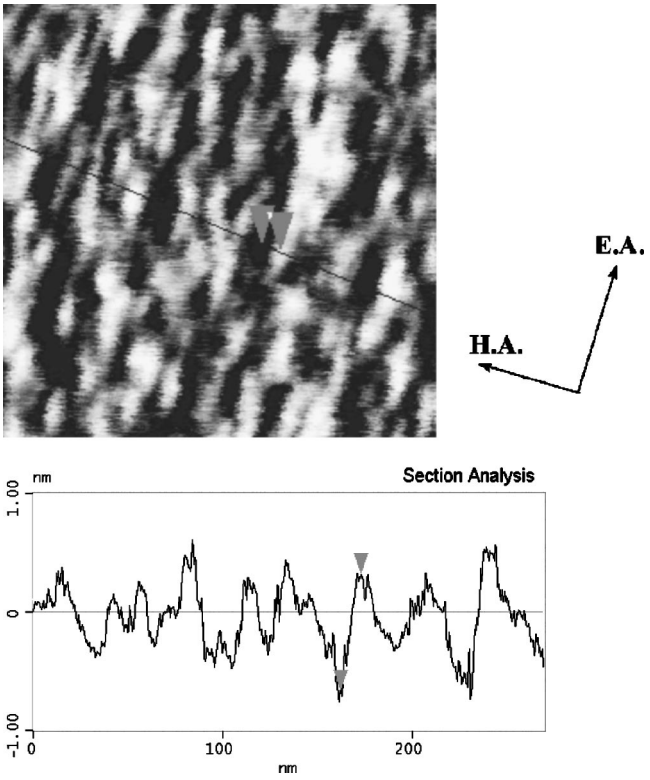

FIG. 1. AFM image showing the topography of the obliquely sputtered 5-nm Ta underlayer. The scan size is 250×250 nm^2. The cross-sectional view shows the profile of the one-dimensional wavelike structure.

saturation magnetization fixed to the value 1400 erg/cm^3. The best fit gives $K_u=(7.6\pm0.04)\times10^5$ erg/cm^3 and $K_s=(2.6\pm0.06)\times10^6$ erg/cm^3. This analysis gives a fitted value of the thickness of the Co layer of 5.5 ± 0.4 nm, and is in reasonable agreement with the nominal value determined using the quartz microbalance. The slightly higher fitted value for the film thickness may originate from the morphological properties of the obliquely sputtered Ta underlayer. The value of K_u gives a uniaxial anisotropy field, $H_k=2K_u/M_s\approx1.0$ kOe, determined by this BLS analysis, and is in very good agreement with the value which can be estimated from the saturation of the HA loops. Although a non-negligible out-of-plane anisotropy has been found, the corresponding out-of-plane anisotropy field of 3.7 ± 0.08 kOe is not high enough to overcome the huge demagnetizing field of approximately 17.6 kOe which aligns the magnetization of the Co layer in the film plane.

The uniaxial anisotropy K_u and saturation field H_{sat} of the SyAF system were studied as a function of top Co layer thickness. Figure 3(a) shows the in-plane angular dependence of the resonance field, H_0, determined from FMR spectra for samples with different top Co layer thickness. The anisotropy field was determined as the difference between the resonance fields measured from the EA ($\Phi=0°$) and HA ($\Phi=\pm90°$) of the sample. The anisotropy field induced by the wavy surface of the Ta underlayer and the exchange coupling through the Ru spacer, was found to be inversely proportional to the top Co layer thickness. In addi-

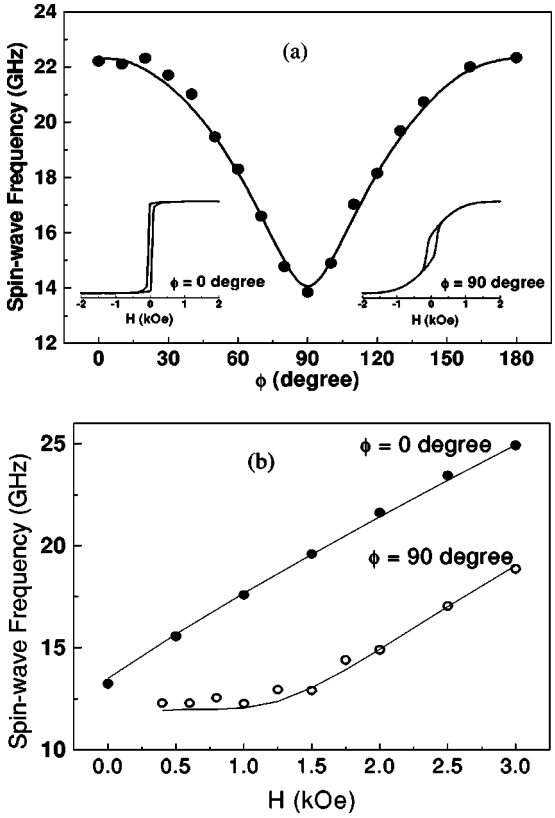

FIG. 2. Dispersion of the Damon-Eshbach mode for Si(100)/Ta (5 nm)/Co (5 nm)/Ta (10 nm) as a function of (a) the in-plane direction of the magnetic field and (b) of the field intensity applied along the easy (full point) and hard (open points) in-plane directions. In all measurements the incidence angle of light is 30°. In (a) and (b) the continuous curve is the result of the fitting procedure. The insets of (a) also show the hysteresis loops measured along the easy- and hard-axis in-plane directions.

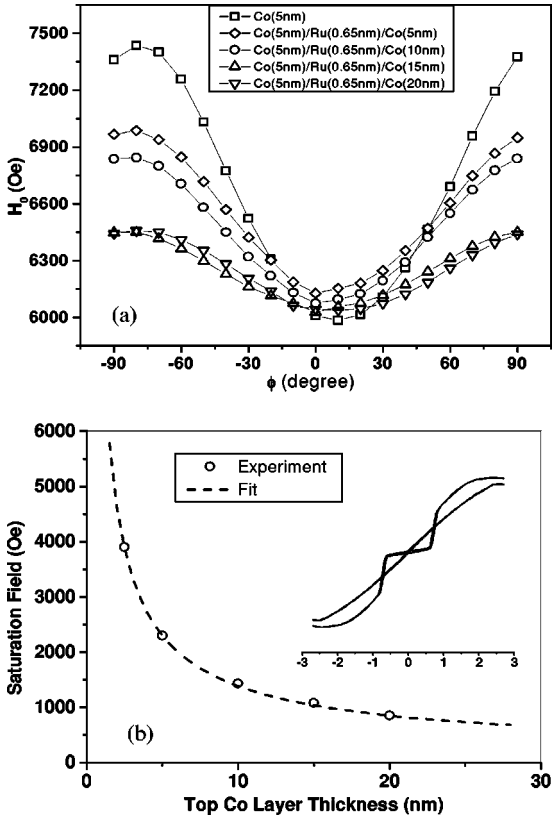

FIG. 3. (a) In-plane angular-dependent resonance field of Si(100)/Ta (5 nm)/Co (5 nm)/Ru (0.65 nm)/Co (t_2)/Ta (10 nm) as a function of top Co layer thickness, t_2. (b) Dependence of easy-axis saturation field H_{sat} on top layer Co thickness. The dashed line is a fit to the model described in the text. The inset shows the hysteresis loop of a symmetrical Co/Ru/Co SyAF structure.

tion, the effective coupling strength was found to be a function of the top ferromagnetic layer thickness. Figure 3(b) shows the easy-axis saturation field H_{sat} as a function of the top layer Co thickness, t_2. Typical magnetization curves, measured both along the in-plane EA and HA, for a symmetrical structure, Co (5 nm)/Ru (0.65 nm)/Co (5 nm), are shown in the inset of Fig. 3(b). In order to obtain a quantitative gauge of the coupling strength dependence on top Co layer thickness, the data is fit to[15]

$$H_{sat} = \frac{1}{2M_s}\left(\frac{1}{t_2} - \frac{1}{t_1}\right)(j_1 + j_2) + \frac{1}{M_s}\sqrt{\left[\frac{1}{2}\left(\frac{1}{t_2} - \frac{1}{t_1}\right)(j_1 + j_2) + 2K_u\right]^2 + \frac{4K_u(j_1 + j_2)}{t_2}}, \quad (1)$$

where M_s is the saturation magnetization for Co, K_u is the induced uniaxial anisotropy of the bottom Co layer, and j_1 and j_2 are the bilinear and biquadratic exchange coupling constants, respectively. We approximate K_u to be equal to its average value to fit the dependence of H_{sat} on top layer thickness. This equation was obtained by an energy minimization calculation of a phenomenological expression for areal energy density in a SyAF structure.[15] A coherent rotation mechanism was assumed in the magnetic reversal process for the SyAF structure. A good agreement with the experimental values for H_{sat} is obtained for $j_1 + j_2 = 0.85$ erg/cm^2. As suggested by a recent magneto-optical indicator film measurement on a Co (2.6 nm)/Ru (0.5 nm)/Co (2.1 nm) trilayer at remanence, where a noncollinear coupling of the two Co layers was observed,[16] the anisotropy and the coupling strength decrease may be attributed to a competition between the antiferromagnetic exchange coupling through the Ru layer and the ferromagnetic coupling from local Co atoms.

Figures 4(a) and 4(b) show the $I_\perp$ MR curves for the samples of Co (5 nm)/Ru (0.65 nm)/Co (5 nm) and Co (5 nm)/Ru (0.65 nm)/Co (20 nm). The higher resistance subpeaks observed in both curves originate from anisotropic magnetoresistance.[17] As the resistance at the peaks is higher with respect to that measured at saturation, where the layer magnetization is uniform and parallel to the H_{ext}, it is possible that the layer magnetization at the peaks is not uniform and may have some components perpendicular to H_{ext}. Both features suggest that the subpeaks of the MR curves originate from Co layers splitting into multiple domains during the magnetization reversal process.

As demonstrated by the direction change of magnetiza-

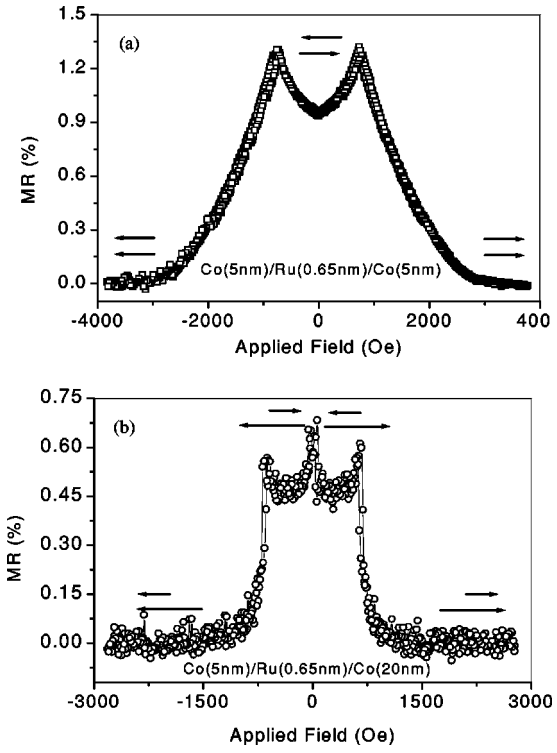

FIG. 4. (a) MR curve of Si(100)/Ta (5 nm)/Co (5 nm)/Ru (0.65 nm)/Co (5 nm)/Ta (10 nm). (b) MR curve of Si(100)/Ta (5 nm)/Co (5 nm)/Ru (0.65 nm)/Co (20 nm)/Ta (10 nm). Both measurements are performed in the $I_{\perp}$ configuration. The arrows show the magnetization direction for the two Co layers.

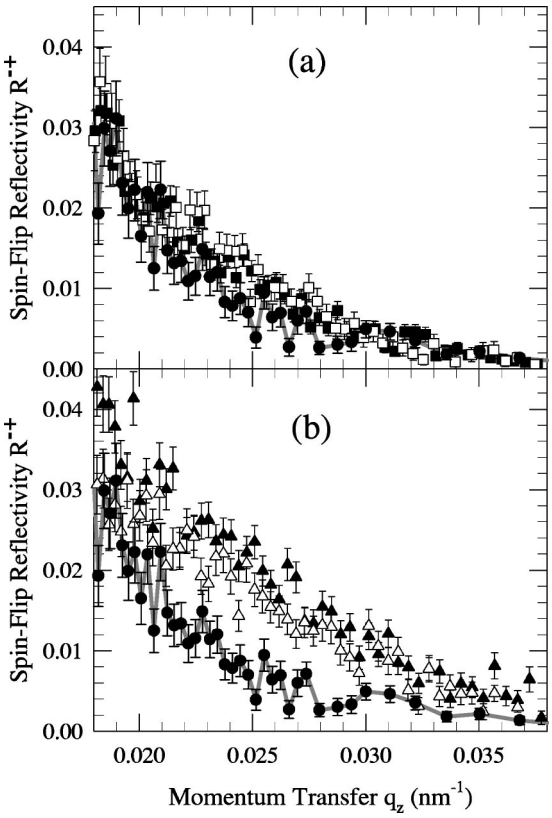

FIG. 5. Spin-flip reflectivity measured on a Co (16 nm)/Ru (0.65 nm)/Co (4.5 nm) sample: At saturation at 3 kOe (filled circle); (a) at AF-ordered states at +200 Oe (filled square) and −200 Oe (open square); (b) During transitions between saturation and AF-ordered state at +600 Oe (filled triangle) and −600 Oe (open triangle). Enhancement of the spin-flip reflectivity during the transitions revealed rotated Co magnetization.

tions of both of the two Co layers in Fig. 4, the magnetization reversal processes occur only at the critical field H_{cr} for the symmetrical structure, whereas reversal occurs at both the critical and coercive fields for the asymmetrical structure. In Fig. 4(b), the center peaks for the asymmetrical SyAF structure are due to the formation of domains within both of the Co layers followed by simultaneous switching of magnetizations, while no similar switching process is necessary for the symmetrical structure. The magnitude of the center subpeaks of the asymmetrical SyAF, at the coercive fields, is also slightly higher than the other two subpeaks. This is due to the fact that both Co layers contribute to MR when they form multiple domains, creating domain walls and reversing magnetizations simultaneously at H_c, while only one Co layer reverses at the critical field on each side.

In a previous study, we reported the use of PNR (Refs. 18–20) to study the magnetization of individual Co layers in different magnetic states on a Co (16 nm)/Ru (0.65 nm)/Co (4.5 nm) SyAF sample.[10] We found the thinner Co layer reversed its magnetization when the system went from saturation to AF-ordered state. PNR can also be used to examine the process by which the Co layer reversed its magnetization during the transition. During the measurements, pulses of polarized neutrons with wavelength λ ranging from 0.2 to 1.4 nm impinge on the sample at a grazing incident angle $\theta \leqslant 1°$. The reflectivity of the neutrons that reverse their polarization ("spin-flip reflectivity") is recorded as a function of the momentum transfer perpendicular to the sample surface, $q_z = 4\pi \sin\theta/\lambda$. The spin-flip reflectivity is caused by magnetic moments that are perpendicular to the applied field direction; its presence during reversal indicates the magnetization reversal process is not a nucleation and growth of domains in the opposition direction. Figure 5 shows the measured spin-flip reflectivity. They were measured at saturation with an applied field of 3 kOe [Figs. 5(a) and 5(b)]; at ±200 Oe when the Co layers are AF ordered [Fig. 5(a)]; at +600 Oe, during the transition from saturation to the AF-ordered state; and during the transition in the opposite directions at −600 Oe [Fig. 5(b)].

At saturation, where both Co layers are magnetized along the applied field, the nonzero intensity in the spin-flip channel is due to the background noises from the limited efficiency of the polarizer, the spin flipper, and the analyzer. At the AF-ordered state at ±200 Oe, the spin-flip reflectivity curves are virtually indistinguishable from those measured at saturation [Fig. 5(a)]. The moments in both Co layers are collinear with the applied field. This result agrees with the results of non-spin-flip PNR measurements in our previous report,[10] where we found the thicker Co layer aligned along the applied field and the thinner Co layer was in the opposite direction. Enhancement of the spin-flip reflectivity was clearly observed during the transitions between saturation

and antiparallel state at ±600 Oe. This spin-flip intensity indicated that there are magnetic moments transverse to the applied field in the thinner Co layer as it reversed its magnetization. The reversal did not occur through a nucleation and growth of magnetic domains in the opposite direction. A comparison with calculated reflectivity also ruled out coherent single-domain rotation as the reversal mechanism. The observed magnetization switching substantiates the results obtained using the magneto-optical indicator film technique for Co (2.6 nm)/Ru (0.5 nm)/Co (2.1 nm) deposited on obliquely sputtered Ta.[16]

In conclusion, Co/Ru/Co SyAF layers were fabricated on obliquely sputtered Ta underlayers. The anisotropic roughness of the obliquely sputtered Ta underlayer was found to be the origin of the uniaxial anisotropy. The magnetic properties depend on the Co layer thickness and the findings reveal large anisotropy fields which create distinct easy- and hard-axis loops. The anisotropy shows that SyAF structures prepared on obliquely sputtered Ta underlayers have potential applications in SV devices. The SV structure can be improved by eliminating the AF pinning layer, which is a source of high resistance in current perpendicular to the plane devices. In addition, the anisotropy field and the coupling strength can be tuned as a function of top Co layer thickness.

This work was supported by the National Science Foundation through the Materials Research Science and Engineering (MRSEC) Center Grant No. DMR-0213985 at the University of Alabama. Oak Ridge National Laboratory is managed for the USDOE by UT-Battelle, LLC under Contract No. DE-AC05-00OR22725. Work at Argonne National Laboratory is supported by US Department of Energy, Office of Science through Contract No. W-31-109-ENG-38.

*Author to whom correspondence should be addressed. Electronic address: gmankey@mint.ua.edu

[1] Yihong Wu, Kebin Li, Jinjun Qiu, Zaibing Guo, and Guchang Han, Appl. Phys. Lett. **80**, 4413 (2002).
[2] Y. Jiang, S. Abe, T. Nozaki, N. Tezuka, and K. Inomata, Appl. Phys. Lett. **83**, 2874 (2003).
[3] D. C. Worledge, Appl. Phys. Lett. **84**, 4559 (2004).
[4] Eric E. Fullerton, D. T. Margulies, M. E. Schabes, M. Carey, B. Gurney, A. Moser, M. Best, G. Zeltzer, K. Rubin, and H. Rosen, Appl. Phys. Lett. **77**, 3806 (2000).
[5] B. Dieny, V. S. Speriosu, S. S. P. Parkin, B. A. Gurney, D. R. Wilhoit, and D. Mauri, Phys. Rev. B **43**, 1297 (1991).
[6] T. G. S. M. Rijks, W. J. M. de Jonge, W. Folkerts, J. C. S. Kools, and R. Coehoorn, Appl. Phys. Lett. **65**, 916 (1994).
[7] R. Moroni, D. Sekiba, F. Buatier de Mongeot, G. Gonella, C. Boragno, L. Mattera, and U. Valbusa, Phys. Rev. Lett. **91**, 167207 (2003).
[8] D. S. Chuang, C. A. Ballentine, and R. C. O'Handley, Phys. Rev. B **49**, 15 084 (1994).
[9] R. D. McMichael, C. G. Lee, J. E. Bonevich, P. J. Chen, W. Miller, and W. F. Egelhoff, Jr., J. Appl. Phys. **88**, 5296 (2000).
[10] Z. Zhao, P. Mani, W.-T. Lee, and G. J. Mankey, J. Appl. Phys. **95**, 7157 (2004).
[11] Richard A. Fry, R. D. McMichael, J. E. Bonevich, P. J. Chen, W. F. Egelhoff Jr., and C.-G. Lee, J. Appl. Phys. **89**, 6825 (2001).
[12] L. Zhou, Z. Zhang, P. E. Wigen, and K. Ounadjela, J. Appl. Phys. **76**, 7078 (1994).
[13] G. Gubbiotti, S. Tacchi, G. Carlotti, G. Socino, F. Spizzo, Z. Zhao, P. Mani, and G. J. Mankey, J. Magn. Magn. Mater. **286**, 468 (2005).
[14] R. W. Damon and J. R. Eshbach, J. Phys. Chem. Solids **19**, 308 (1961).
[15] K. Zhang, T. Kai, T. Zhao, H. Fujiwara, and G. J. Mankey, J. Appl. Phys. **89**, 6814 (2001).
[16] V. S. Gornakov, V. I. Nikitenko, W. F. Egelhoff, R. D. McMichael, A. J. Shapiro, and R. D. Shull, J. Appl. Phys. **91**, 8272 (2002).
[17] *Ferromagnetic Materials*, edited by E. P. Wohlfarth (North-Holland, Amsterdam 1982), Vol. 3, p. 747.
[18] J. F. Ankner and G. P. Felcher, J. Magn. Magn. Mater. **200**, 741 (1999).
[19] C. F. Majkrzak, Physica B **221**, 342 (1996).
[20] H. Zabel, R. Siebrecht, and A. Schreyer, Physica B **276**, 17 (2000).